ELSEVIER

Journal of Chromatography A, 777 (1997) 295–309

JOURNAL OF CHROMATOGRAPHY A

Dry look at the CHARM (charged resolving agent migration) model of enantiomer separations by capillary electrophoresis

Billy A. Williams, Gyula Vigh*

Chemistry Department, Texas A&M University, College Station, TX 77843-3255, USA

Received 30 December 1996; revised 25 March 1997; accepted 15 April 1997

Abstract

An analysis of the capillary electrophoretic separation of enantiomers using permanently charged cyclodextrins as resolving agents is presented. The charged resolving agent migration model (CHARM model) is based on the consideration of the simultaneous protonation and 1:1-type complexation equilibria that take place in such background electrolytes. Analytical expressions are derived that allow the calculation of the effective charge, effective mobility, separation selectivity and peak resolution values for various enantiomeric analyte classes: non-electrolytes, strong electrolytes and weak electrolytes. Analysis of the resulting surfaces as a function of the pH and the charged cyclodextrin concentration of the background electrolyte indicates that, in the absence of electroosmotic flow (e.g. in neutral-coated capillaries), only two series of measurements have to be carried out to locate the best separation conditions as a function of the concentration of the charged cyclodextrin: one in low-pH background electrolytes (e.g. pH 2.2) and one in high-pH background electrolytes (e.g. pH 9.5 or above). By taking advantage of the predictions of the CHARM model, the utility of a large number of charged cyclodextrins, each offering different intermolecular (enantioselective) interactions can be evaluated in a short period of time for any chiral analyte. © 1997 Elsevier Science B.V.

Keywords: Enantiomer separation; Charged resolving agent migration

1. Introduction

Capillary electrophoretic enantiomer separations have had a spectacular career: after an early start as academic curiosities they have become, in less than a decade, reliable tools in the hands of separation scientists. This progress is well documented in up-to-date, excellent reviews [1,2]. Recently, the successful use of charged cyclodextrins (CCDs), both weak electrolyte derivatives, e.g. [3–5], and strong electrolyte derivatives, e.g. [6–13], generated great interest in the exploration of the potentials of these chiral resolving agents. Though several background electrolyte (BE) parameters including the type and concentration of the resolving agent, the pH and organic modifier concentration of the BE and the electroosmotic (EO) flow-rate were either intentionally or unavoidably varied in these investigations, a comprehensive picture firmly grounded in solution equilibria, similar to what is available for non-charged chiral resolving agents (e.g. [14–23]), has not been published yet. Experimental difficulties involved with the use of CCDs, such as (i) the fact that most commercially available materials are complicated mixtures which contain a large number of isomers, (ii) the great changes in ionic strength as

*Corresponding author.

PII S0021-9673(97)00424-X

the concentration of the CCD in the BE is varied, and (iii) the lack of a method that can be used to measure accurate EO flow-rates in the presence of CCDs (which can complex with the EO flow markers) prevented the determination of meaningful complexation constants and delayed modeling. This is unfortunate, because an analysis of what could be expected from the use of CCDs under ideal conditions could shed light on the experimental variables and the range of their values that need to be controlled or exploited to achieve separation. The objective of this paper is to provide such an analysis and derive a set of guidelines to help the facile optimization of CE enantiomer separations which rely on the use of CCDs. This will be done by looking at the characteristics of the charged resolving agent migration model, the CHARM model. Since no actual experimental data will be discussed in the analysis (though the equilibrium constant and mobility data used in the calculations are perceived to be realistic), this attempt is termed a 'dry' look at the problem, and it is hoped that experimental means will soon be developed to measure ionic mobilities and complexation constants. Since the equilibrium expressions are far simpler for noncharged and monocharged analytes in 1:1-type complexes, only these will be discussed. Nevertheless, *mutatis mutandis*, the general principles and lessons learned for these simple analytes can be applied for multiply-charged analytes involved in higher-order complexation as well.

Successful enantiomer separations depend on a large number of variables: instrumental, operational and compositional. Instrumental and operational variables (instrumentation-related peak dispersion, separation potential, power dissipation, temperature control) are generally adequately and predictably controlled in most modern instruments. However, at our current level of understanding, only some of the compositional variables of the background electrolyte (such as pH, concentration and charge of the resolving agent, effective charge of the analyte and EO flow-rate) have predictable effects. Other compositional variables (such as the structure of the resolving agent, the organic co-solvent and/or the other additives) cause great, but unpredictable changes. This paper will deal only with the former, predictable aspects of methods development.

2. Discussion

2.1. Generalized peak resolution equation

Previously, by considering an ideal CE system (where peak dispersion is caused only by longitudinal diffusion), Friedl and Kenndler [24] derived a general expression that relates peak resolution, R_s, to the Boltzman constant, k, the electric charge, e_0, the absolute temperature, T, the length of the capillary, l, the electric field strength, E, the effective charge of the solutes, z_i^{eff}, and the separation selectivity, α. They defined separation selectivity for components 1 and 2 as:

$$\alpha = \frac{\mu_1^{\text{eff}}}{\mu_2^{\text{eff}}} \tag{1}$$

where the effective mobility of component i, μ_i^{eff}, was calculated from the observed mobility, μ_i^{obs}, and the EO mobility, μ_{eo}, as:

$$\mu_i^{\text{obs}} = \mu_i^{\text{eff}} + \mu_{\text{eo}} \tag{2}$$

Their approach was extended in [19] to include the effects of the EO flow as well, yielding the following peak resolution expression:

$$R_s = \sqrt{\frac{Ele_0}{8kT}} \times \frac{\text{abs}(\alpha - 1)\sqrt{\text{abs}(\alpha + \beta)}\sqrt{\text{abs}(1 + \beta)}\sqrt{z_1^{\text{eff}}}\sqrt{z_2^{\text{eff}}}}{\sqrt{\text{abs}((\alpha + \beta)^3)\, z_1^{\text{eff}}} + \sqrt{\alpha\ \text{abs}((1 + \beta)^3)\, z_2^{\text{eff}}}} \tag{3}$$

where the normalized EO mobility, β, is:

$$\beta = \frac{\mu_{\text{eo}}}{\mu_2^{\text{eff}}} \tag{4}$$

Eq. (3) is the key to the rational development of enantiomer separations in CE. By varying β independently (e.g. by using coated capillaries with well-defined EO flow characteristics), R_s can be readily optimized if the dependence of α, z_1^{eff} and z_2^{eff} on the compositional variables of the BE is known.

2.2. Generalized equilibrium model yielding z^{eff}, μ^{eff} and α

Since direct enantiomer separations in free solution CE rely on the differential binding of the analyte

enantiomers to at least one chiral resolving agent dissolved in the BE, multiple chemical equilibria will be established which govern the effective charge and effective mobility of the analytes. The appropriate multiple equilibrium expressions can then be combined with the appropriate mass balance equations to obtain a set of mole fraction function expressions for all analyte species coexisting in the BE. When these expressions are combined with the Tiselius relationships [25], the effective charge of the analyte can be obtained as the linear combination of the ionic charges and the mole fractions of the species involved, and the effective mobility of the analyte can be obtained as the linear combination of the ionic mobilities and the mole fractions of the species involved.

Generally, in the CE separation of enantiomers, CCDs can complex with both the BE components and the analytes. When the concentrations of the BE constituents and the CCD are much higher than those of the analytes, the concentration of the governing form of the CCD remains practically the same, whether analytes are present or not. Therefore, in first approximation, the equilibria between CCD and the BE constituents can be omitted from formal consideration.

Since both enantiomers of the analyte, R and S, participate in similar equilibria, expressions will only be shown for the R enantiomer. Initially, formal protonation and complexation reactions will be written for R, regardless of its actual chemical structure (strong or weak electrolyte, negatively charged, noncharged or positively charged analyte). The resulting general expressions will be simplified as they are applied for the typical analyte families.

The protonation and complexation reactions for the R enantiomer are:

$$R + H_3O^+ \rightleftarrows HR + H_2O \tag{5}$$

$$R + CD \rightleftarrows RCD \tag{6}$$

$$HR + CD \rightleftarrows HRCD \tag{7}$$

with the corresponding equilibrium expressions as:

$$K = \frac{[HR]}{[R][H_3O^+]} \tag{8}$$

$$K_{RCD} = \frac{[RCD]}{[R][CD]} \tag{9}$$

$$K_{HRCD} = \frac{[HRCD]}{[HR][CD]} \tag{10}$$

The mass balance equation for the R enantiomer is:

$$c_R = [R] + [HR] + [RCD] + [HRCD] \tag{11}$$

where c_R is the analytical concentration of R. The respective mole fractions,

$$\phi_R = \frac{[R]}{c_R} \tag{12}$$

$$\phi_{HR} = \frac{[HR]}{c_R} \tag{13}$$

$$\phi_{RCD} = \frac{[RCD]}{c_R} \tag{14}$$

$$\phi_{HRCD} = \frac{[HRCD]}{c_R} \tag{15}$$

can be obtained from Eqs. (8)–(13) as:

$$\phi_R = \frac{1}{1 + K_{RCD}[CD] + K[H_3O^+](1 + K_{HRCD}[CD])} \tag{16}$$

$$\phi_{HR} = \frac{K[H_3O^+]}{1 + K_{RCD}[CD] + K[H_3O^-](1 + K_{HRCD}[CD])} \tag{17}$$

$$\phi_{RCD} = \frac{K_{RCD}[CD]}{1 + K_{RCD}[CD] + K[H_3O^-](1 + K_{HRCD}[CD])} \tag{18}$$

$$\phi_{HRCD} = \frac{K[H_3O^+]K_{HRCD}[CD]}{1 + K_{RCD}[CD] + K[H_3O^+](1 + K_{HRCD}[CD])} \tag{19}$$

The effective charge of the R enantiomer is obtained as the linear combination of the mole fractions (ϕ_i) and the ionic charges (z_i^0) of the related species [25]:

$$z_R^{eff} = z_R^0\phi_R + z_{HR}^0\phi_{HR} + z_{RCD}^0\phi_{RCD} + z_{HRCD}^0\phi_{HRCD} \quad (20)$$

The effective mobility of the R enantiomer is obtained as the linear combination of the mole fractions (ϕ_i) and ionic mobilities (μ_i^0) of the related species [25]:

$$\mu_R^{eff} = \mu_R^0\phi_R + \mu_{HR}^0\phi_{HR} + \mu_{RCD}^0\phi_{RCD} + \mu_{HRCD}^0\phi_{HRCD} \quad (21)$$

By combining Eqs. (16)–(21), z^{eff} and μ^{eff} of R are obtained as:

$$z_R^{eff} = \frac{z_R^0 + z_{RCD}^0 K_{RCD}[CD] + K[H_3O^+](z_{HR}^0 + z_{HRCD}^0 K_{HRCD}[CD])}{1 + K_{RCD}[CD] + K[H_3O^+](1 + K_{HRCD}[CD])} \quad (22)$$

and

$$\mu_R^{eff} = \frac{\mu_R^0 + \mu_{RCD}^0 K_{RCD}[CD] + K[H_3O^+](\mu_{HR}^0 + \mu_{HRCD}^0 K_{HRCD}[CD])}{1 + K_{RCD}[CD] + K[H_3O^+](1 + K_{HRCD}[CD])} \quad (23)$$

Since similar expressions are obtained for the S enantiomer, separation selectivity, α (Eq. (1)), becomes:

$$\alpha = \frac{\mu_R^0 + \mu_{RCD}^0 K_{RCD}[CD] + K[H_3O^+](\mu_{HR}^0 + \mu_{HRCD}^0 K_{HRCD}[CD])}{\mu_S^0 + \mu_{SCD}^0 K_{SCD}[CD] + K[H_3O^+](\mu_{HS}^0 + \mu_{HSCD}^0 K_{HSCD}[CD])} \times \frac{1 + K_{SCD}[CD] + K[H_3O^+](1 + K_{HSCD}[CD])}{1 + K_{RCD}[CD] + K[H_3O^+](1 + K_{HRCD}[CD])} \quad (24)$$

Effective analyte charge, effective analyte mobility and separation selectivity all depend on the ionic mobilities of both the free and the complexed species, the protonation constant, the complex formation constants of both the ionic and the nonionic forms of the enantiomers, as well as the pH and the CD concentration of the BE. If the K, z^0 and μ^0 values are available, the theoretical peak resolution values can be calculated with Eq. (3) and Eqs. (22)–(24).

The power of the equilibrium approach lies in the realization that Eq. (3), Eq. (23) and Eq. (24) can be applied to different solute classes (strong vs. weak electrolytes, acids vs. bases, charged vs. noncharged resolving agents, etc.) and the characteristic resolution surfaces can be calculated with K, z^0 and μ^0 values which are presumed to be realistic for these kinds of separations (moderate binding strengths, moderate ionic mobilities, enantiomer binding constants and mobilities differing by about 10%). These theoretical resolution surfaces can in turn be analyzed and generally applicable analytical conditions and optimization protocols can be derived for the solute classes considered. Since enantiomer separations which rely on noncharged chiral resolving agents have been treated by this approach in detail [17–22], only the use of charged resolving agents will be discussed here.

2.3. Enantiomer separations using charged chiral resolving agents

Charged resolving agents have the unique advantage that they can be used for the separation of both noncharged and charged analyte enantiomers. CCDs can carry either strong electrolyte functional groups (such as sulfate, sulfobutyl ether, sulfopropyl ether or tetraalkylammonium groups), or weak electrolyte functional groups (such as carboxymethyl, carboxyethyl, phosphate or amino groups). CDs with strong electrolyte functional groups are generally preferable, because then the pH of the BE can be adjusted freely according to the needs of the analyte, without effecting the native charge of the resolving agent. Cyclodextrins derivatized with weak electrolyte functional groups offer an advantage when they provide unique, otherwise not available intermolecular interactions.

Since it is expected that the much-desired single-isomer CCDs (or other single-isomer chiral resolving agents) will become commercially available sooner or later, and since theory-based conclusions can only be drawn for such materials, this paper presumes the use of single-isomer strong electrolyte chiral resolving agents. Eq. (3) predicts that, everything else being equal, R_s improves with the square-root of the effective charge. Therefore, a hypothetical cyclodextrin, fully substituted with charged functional groups on its nonchiral face will be used in the calculations. The analytes discussed will be, successively, noncharged species, singly-charged permanent ions and, finally, monoprotic weak electrolytes.

The R_s surfaces calculated with Eq. (3) for two

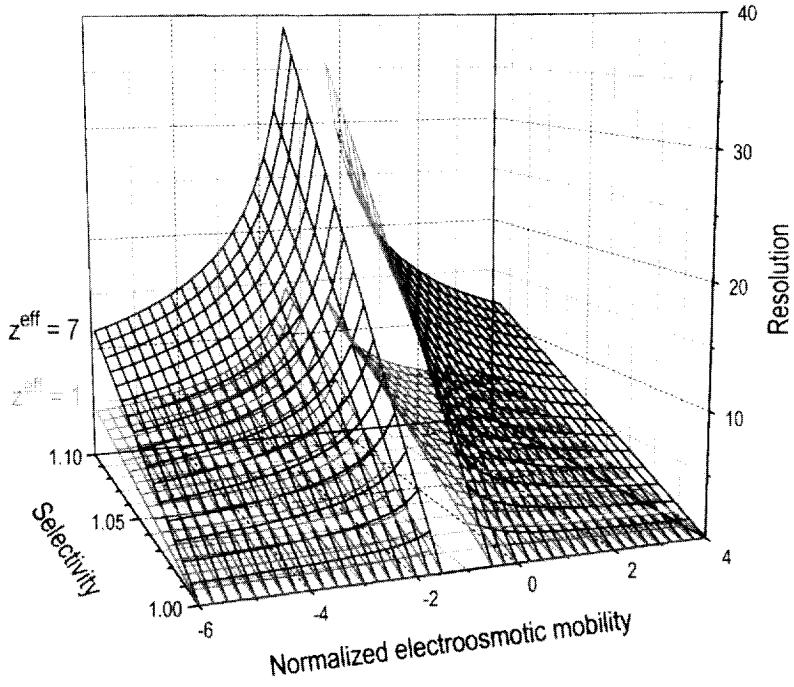

Fig. 1. Peak resolution as a function of separation selectivity (α) and the normalized electroosmotic mobility (β) for a monocharged analyte ($z^{eff}=1$) and a seven-charged analyte ($z^{eff}=7$). Constants used for the calculation: $z_1^{eff}=z_2^{eff}=1$ and $z_1^{eff}=z_2^{eff}=7$, $(e_0/8k)^{1/2}=38.0868$, $E=500$ V/cm, $l=19.5$ cm, $T=310$ K.

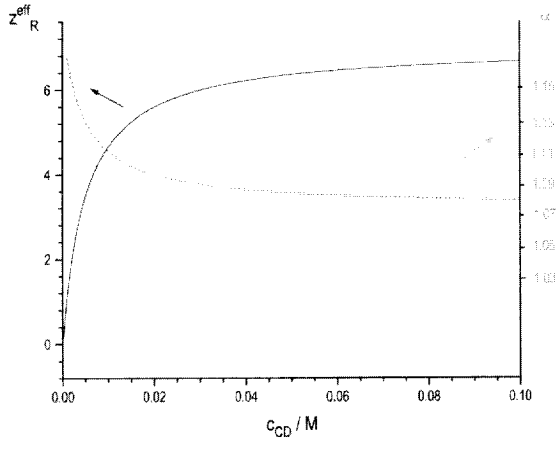

Fig. 2. Effective charge (solid line, left axis) and separation selectivity (dotted line, right axis) for a non-electrolyte enantiomer as a function of the CCD concentration of the BE. Constants used for the calculation: $z^0_{RCD}=z^0_{SCD}=7$, $\mu^0_{RCD}=25\times10^{-5}$ cm^2/Vs, $\mu^0_{SCD}=27\times10^{-5}$ cm^2/Vs, $K_{RCD}=200$ and $K_{SCD}=220$.

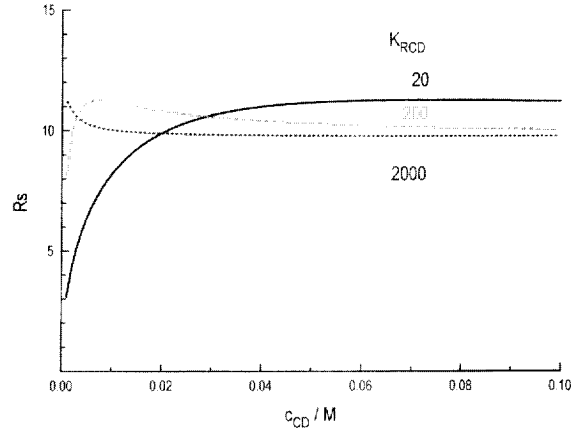

Fig. 3. Peak resolution for a non-electrolyte enantiomer pair as a function of the CCD concentration of the BE at different complexation strengths. Constants used for the calculation: $z^0_{RCD}=z^0_{SCD}=7$, $\mu^0_{RCD}=25\times10^{-5}$ cm^2/Vs, $\mu^0_{SCD}=27\times10^{-5}$ cm^2/Vs, $(e_0/8k)^{1/2}=38.0868$, $E=100$ V/cm, $l=19.5$ cm, $T=310$K and $\beta=0$. Solid curve: $K_{RCD}=20$, $K_{SCD}=22$. Dashed curve: $K_{RCD}=200$, $K_{SCD}=220$. Dotted curve: $K_{RCD}=2000$, $K_{SCD}=2200$.

limiting effective charges, $z^{eff}=1$ and $z^{eff}=7$, are shown as a function of the separation selectivity, α, and the normalized EO mobility, β, in Fig. 1. As a reasonable approximation, it was assumed in the calculation of these surfaces that $z_1^{eff}=z_2^{eff}$. Everything else being equal, the higher z^{eff}, the greater R_s. When z^{eff} and β are held constant, R_s increases almost linearly with α. R_s depends very sensitively on β. Discontinuities develop in R_s as the $\beta=-1$ and $\beta=-\alpha$ conditions are approached. As long as $\alpha\neq 1$ and $z^{eff}\neq 0$, R_s can be manipulated widely by adjusting β, though naturally at the expense of varying separation time. If R_s is high due to favorable α and z^{eff} values, the separation speed can always be increased by increasing the absolute value of β.

2.3.1. Separation of non-electrolyte enantiomers with charged chiral resolving agents

For non-electrolyte enantiomers, K, K_{HRCD}, z_R^0, z_{HR}^0, z_{HRCD}^0, μ_R^0, μ_{HR}^0 and μ_{HRCD}^0 are zero. Therefore, the expressions obtained from Eqs. (22)–(24) for z^{eff}, μ^{eff} and α are very simple, and R_s can be predicted easily:

$$z_R^{eff}=\frac{z_{RCD}^0 K_{RCD}[CD]}{1+K_{RCD}[CD]} \tag{25}$$

$$\mu_R^{eff}=\frac{\mu_{RCD}^0 K_{RCD}[CD]}{1+K_{RCD}[CD]} \tag{26}$$

$$\alpha=\frac{\mu_{RCD}^0 K_{RCD}}{\mu_{SCD}^0 K_{SCD}}\,\frac{1+K_{SCD}[CD]}{1+K_{RCD}[CD]} \tag{27}$$

The z^{eff} and α curves calculated with complex formation constant and ionic mobility values presumed to be realistic are shown in Fig. 2. Both z^{eff} and μ^{eff} increase with increasing concentration of the CCD (left axis in Fig. 2). The greater the complexation constant, the more rapidly the limiting values are approached. The α curve (right axis in Fig. 2) also approaches a limiting value as c_{CD} increases. Eq. (27) indicates that at very low CCD concentrations α depends only on the numeric values of the μ_{RCD}^0 and K_{RCD} and μ_{SCD}^0 and K_{SCD} constant pairs. Obviously, α is not defined for $c_{CD}=0$, because no complex can exist there. It is interesting to note that, contrary to superficial intuition, the lower the CCD concentration, the greater the α value.

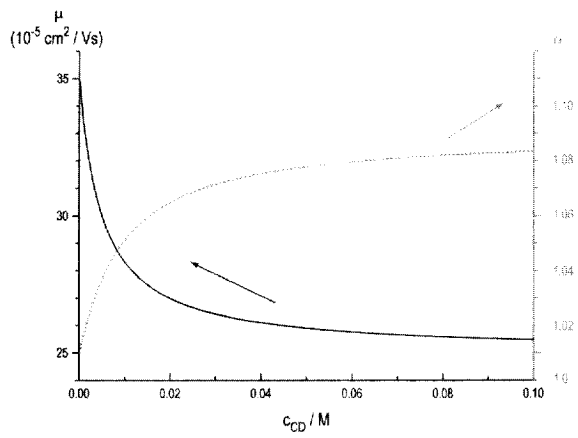

Fig. 4. Effective mobility (solid line, left axis) and separation selectivity (dotted line, right axis) for a strong electrolyte enantiomer pair as a function of the CCD concentration of the BE when the signs of the electric charges are identical. Constants used for the calculation: $z_R^0=z_S^0=1$, $z_{RCD}^0=z_{SCD}^0=8$, $\mu_R^0=\mu_S^0=35\times10^{-5}$ cm^2/Vs, $\mu_{RCD}^0=25\times10^{-5}$ cm^2/Vs, $\mu_{SCD}^0=27\times10^{-5}$ cm^2/Vs, $K_{RCD}=200$, $K_{SCD}=220$.

The corresponding R_s curve ($K_{RCD}=200$, long dashed line) is shown in Fig. 3. Since z^{eff} increases and α decreases with increasing c_{CD}, the R_s curve

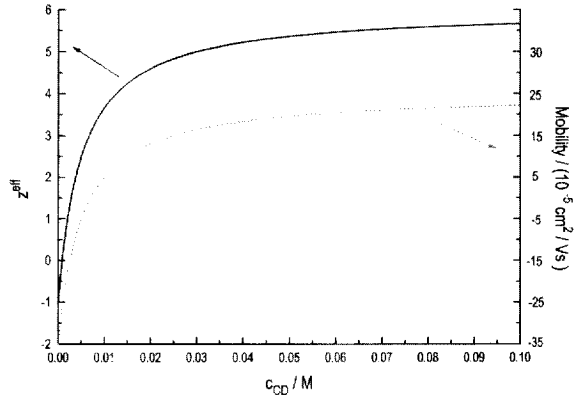

Fig. 5. Effective charge (solid curve, left axis) and effective mobility (dotted curve, right axis) for a strong electrolyte enantiomer pair as a function of the CCD concentration of the BE when the signs of the electric charges are opposite. Constants used for the calculation: $z_R^0=z_S^0=-1$, $z_{RCD}^0=z_{SCD}^0=6$, $\mu_R^0=\mu_S^0=-35\times10^{-5}$ cm^2/Vs, $\mu_{RCD}^0=25\times10^{-5}$ cm^2/Vs, $\mu_{SCD}^0=28\times10^{-5}$ cm^2/Vs, $K_{RCD}=200$, $K_{SCD}=220$.

must show a shallow maximum. It is instructive to see what happens to R_s when the chiral binding constant ratios are kept identical ($K_{RCD}/K_{SCD}=1.1$), but the K values are changed over two orders of magnitude to cover very different complexation strengths ranging from very weak binding ($K_{RCD}=20$, solid lines in Fig. 3), through average binding ($K_{RCD}=200$, long dashed lines in Fig. 3) to very strong binding ($K_{RCD}=2000$, dotted lines in Fig. 3). When K_{RCD} is very low, the maximum occurs at very high CCD concentrations. When K_{RCD} is very high, the maximum occurs at very low CCD concentrations.

Resolution optimization (in the absence of EO flow) is very simple: the highest CCD concentration that (still) provides adequate R_s should be used resulting in the shortest analysis time and the most rugged separation. When needed, one can fine-tune the separation by adjusting the concentration of the CCD to operate at the R_s maximum.

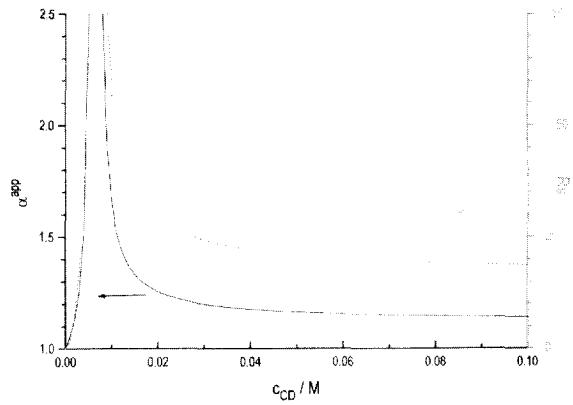

Fig. 6. Separation selectivity and peak resolution for the separation of a strong electrolyte enantiomer pair as a function of the CCD concentration of the BE when the signs of the electric charges are opposite. Constants used for the calculation: $z_R^0=z_S^0=-1$, $z_{RCD}^0=z_{SCD}^0=6$, $\mu_R^0=\mu_S^0=-35\times10^{-5}$ cm^2/Vs, $\mu_{RCD}^0=25\times10^{-5}$ cm^2/Vs, $\mu_{SCD}^0=28\times10^{-5}$ cm^2/Vs, $K_{RCD}=200$, $K_{SCD}=220$, $(e_0/8k)^{1/2}=38.0868$, $E=100$ V/cm, $l=19.5$ cm, $T=310$ K and $\beta=0$.

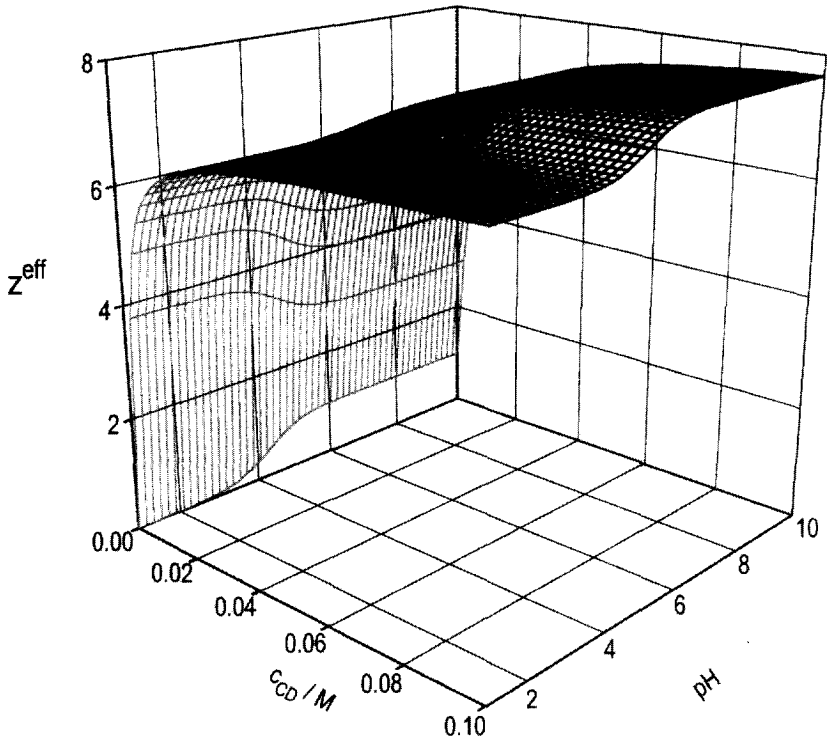

Fig. 7. Effective charge surface for a weak acid enantiomer as a function of the CCD concentration and pH of the BE. Constants used for the calculation: $z_R^0=1$, $z_{RCD}^0=8$, $z_{HRCD}^0=7$, $K_{RCD}=200$, $K_{HRCD}=600$, $K_a=5\times10^{-5}$.

2.3.2. Separation of strong electrolyte enantiomers with charged chiral resolving agents

For strong electrolyte enantiomers, K, K_{HRCD}, z^0_{HR}, z^0_{HRCD}, μ^0_{HR} and μ^0_{HRCD} are zero, $z^0_R = z^0_S = z^0$, $z^0_{RCD} = z^0_{SCD}$ and $\mu^0_R = \mu^0_S = \mu^0$. With these, the z^{eff}, μ^{eff} and α expressions read as:

$$z_R^{eff} = \frac{z^0 + z^0_{RCD}K_{RCD}[CD]}{1 + K_{RCD}[CD]} \quad (28)$$

$$\mu_R^{eff} = \frac{\mu^0 + \mu^0_{RCD}K_{RCD}[CD]}{1 + K_{RCD}[CD]} \quad (29)$$

$$\alpha = \frac{\mu^0 + \mu^0_{RCD}K_{RCD}[CD]}{\mu^0 + \mu^0_{SCD}K_{SCD}[CD]} \frac{1 + K_{SCD}[CD]}{1 + K_{RCD}[CD]} \quad (30)$$

The primary factor to consider in the discussion of Eqs. (28)–(30) is the sign of the z^0_{RCD}/z^0_R ratio, which leads to two different cases.

2.3.2.1. $z^0_{RCD}/z^0_R > 0$

When $z^0_{RCD}/z^0_R > 0$ (the charge of the analyte has the same sign as that of the resolving agent, i.e. separation of a cationic analyte with a cationic CD or separation on an anionic analyte with an anionic CD), abs(z^{eff}) always increases towards the limiting value of 8 as c_{CD} is increased. The effective mobility curves can take two different shapes depending on the value of the μ^0_{RCD}/μ^0_R ratio. When $\mu^0_{RCD}/\mu^0_R < 1$, the effective mobility of the analyte decreases as c_{CD} increases (full line in Fig. 4, left axis); when $\mu^0_{RCD}/\mu^0_R > 1$, the effective mobility of the analyte increases as c_{CD} increases. Since α is obtained as the multiple of two opposing terms, α can increase, decrease or pass through a maximum depending on the numeric values of μ^0_{RCD}/μ^0, μ^0_{SCD}/μ^0 and K_{RCD}/K_{SCD}. In the absence of experimental data for CCDs, Fig. 4 shows the α curve corresponding to the case when $\mu^0_{RCD}/\mu^0_R < 1$, $\mu^0_{RCD}/\mu^0_{SCD} > 1$ and $K_{RCD}/K_{SCD} > 1$. Both abs(z^{eff}) and α increase towards their limiting values

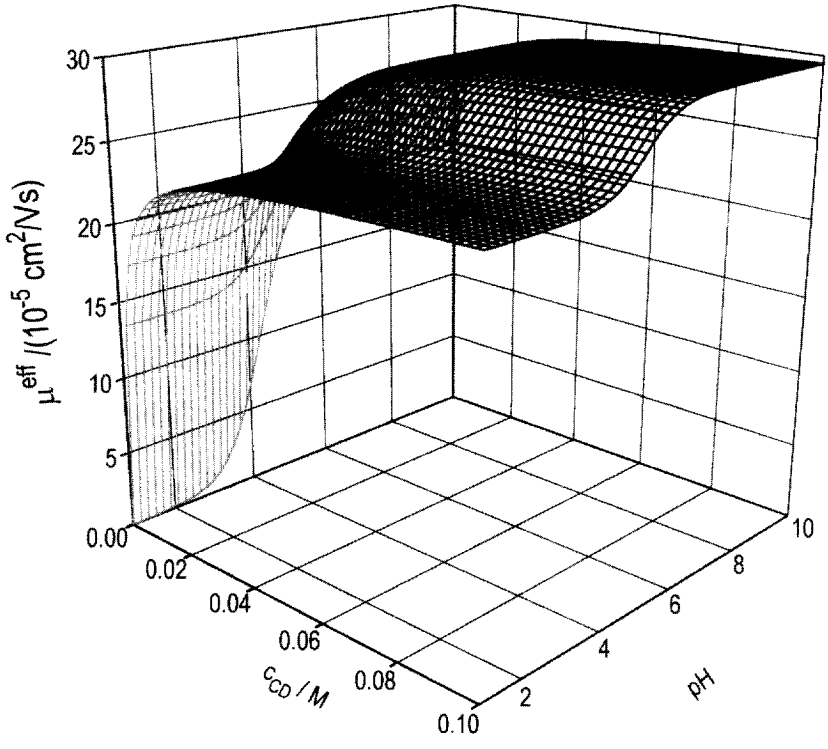

Fig. 8. Effective mobility surface for a weak acid enantiomer as a function of the CCD concentration and pH of the BE. Constants used for the calculation: $\mu^0_R = 20\times10^{-5}$ cm^2/Vs, $\mu^0_{RCD} = 30\times10^{-5}$ cm^2/Vs, $\mu^0_{HRCD} = 25\times10^{-5}$ cm^2/Vs, $K_{RCD} = 200$, $K_{HRCD} = 600$, $K_a = 5\times10^{-5}$.

as the concentration of the CCD is increased, consequently peak resolution will also increase. This makes optimization very simple: the highest c_{CD} will result in the best resolution, the fastest and the most rugged separation. When $\mu^0_{RCD}/\mu^0_R > 1$ and all other values are as in Fig. 4, the α curve remains similar: both α and R_s increase to the limiting values as the CCD concentration is increased.

2.3.2.2. $z^0_R/z^0_{RCD} < 0$

When $z^0_R/z^0_{RCD} < 0$ (the sign of the analyte charge is opposite to that of the chiral resolving agent, i.e. cationic analyte with anionic CD or anionic analyte with cationic CD), z^{eff} changes sign and its absolute value approaches 6, the limiting value, as c_{CD} is increased (solid line, left axis in Fig. 5). The smaller the K, the slower z^{eff} approaches 6. In principle, the μ^{eff} curves can take two different shapes depending on the value of the abs(μ^0_{RCD}/μ^0_R) ratio. When abs(μ^0_{RCD}/μ^0_R) < 1, the effective mobility changes sign and its absolute value decreases as c_{CD} increases (dotted line, right axis in Fig. 5); when abs(μ^0_{RCD}/μ^0_R) > 1, the effective mobility changes sign and its absolute value increases as c_{CD} increases. The α and R_s curves corresponding to Fig. 5 are plotted in Fig. 6. A discontinuity develops in both α (solid line, left axis) and R_s (dotted line, right axis) at a CCD concentration where the μ^{eff}_R/μ^{eff}_S ratio becomes negative, because as the direction of the electrophoretic migration of the two enantiomers becomes opposite, one of the enantiomers never reaches the detector. Once the μ^{eff}_R/μ^{eff}_S ratio becomes positive again at higher CCD concentrations, the two enantiomers migrate in the same direction, albeit with a reversed migration order. R_s can be increased tremendously in the vicinity of this c_{CD} value at the expense of the ruggedness of the separation and greatly increased run time.

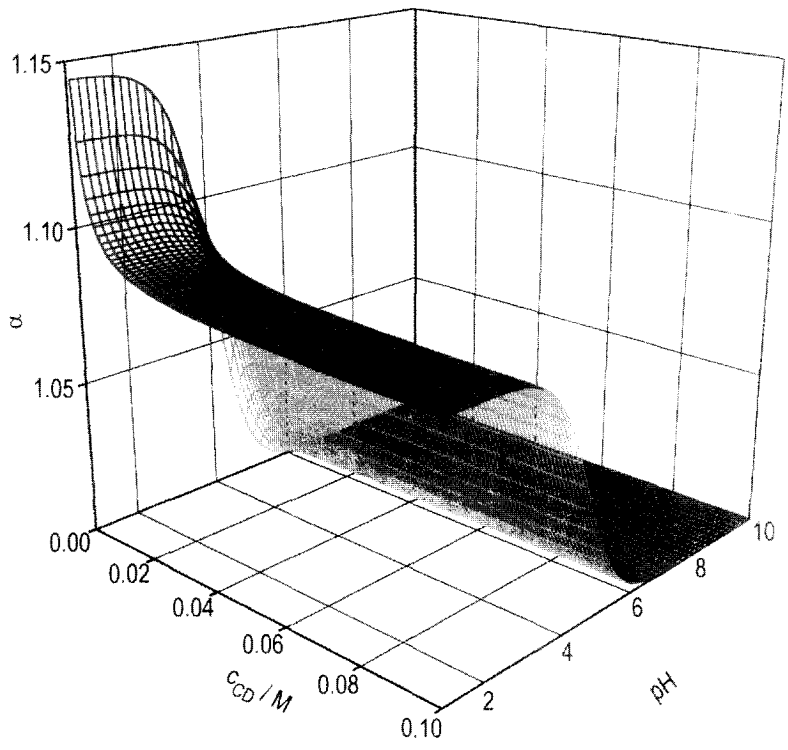

Fig. 9. Separation selectivity surface for a weak acid enantiomer pair as a function of the CCD concentration and pH of the BE, when the separation is desionoselective. Constants used for the calculation: $\mu^0_R = \mu^0_S = 20\times10^{-5}$ cm^2/Vs, $\mu^0_{RCD} = \mu^0_{SCD} = 30\times10^{-5}$ cm^2/Vs, $\mu^0_{HRCD} = 25\times10^{-5}$ cm^2/Vs, $\mu^0_{HSCD} = 27\times10^{-5}$ cm^2/Vs, $K_{RCD} = K_{SCD} = 200$, $K_{HRCD} = 600$, $K_{HSCD} = 660$, $K_a = 5\times10^{-5}$.

2.3.3. Separation of weak electrolyte enantiomers with charged chiral resolving agents

For weak electrolytes, z^{eff}, μ^{eff}, α and R_s depend on both the CCD and the hydronium ion concentration of the BE. Eqs. (22)–(24) can be simplified only slightly, because only z_R^0 and μ_R^0 are zero for weak bases, and z_{HR}^0 and μ_{HR}^0 are zero for weak acids. Eqs. (22)–(24) assume more familiar forms when the protonation constant, K, is replaced by the acid dissociation constant, K_a or the base dissociation constant, K_b. (Note that $K_a = 1/K$ and $K_b = K_w K$, where K_w is the ion product of water.) The z^{eff}, μ^{eff}, α and R_s surfaces for the weak base enantiomers are mirror images of those for the weak acid enantiomers (mirrored around the pH 7 point). Therefore, in the next section, only the behavior of weak acid enantiomers will be discussed.

For weak acid enantiomers, the z^{eff}, μ^{eff} and α expressions read as:

$$z_R^{eff} = \frac{z_R^0 + z_{RCD}^0 K_{RCD}[CD] + z_{HRCD}^0 \dfrac{[H_3O^+]}{K_a} K_{HRCD}[CD]}{1 + K_{RCD}[CD] + \dfrac{[H_3O^+]}{K_a}(1 + K_{HRCD}[CD])} \quad (31)$$

$$\mu_R^{eff} = \frac{\mu_R^0 + \mu_{RCD}^0 K_{RCD}[CD] + \mu_{HRCD}^0 \dfrac{[H_3O^+]}{K_a} K_{HRCD}[CD]}{1 + K_{RCD}[CD] + \dfrac{[H_3O^+]}{K_a}(1 + K_{HRCD}[CD])} \quad (32)$$

$$\alpha = \frac{\mu_R^0 + \mu_{RCD}^0 K_{RCD}[CD] + \mu_{HRCD}^0 \dfrac{[H_3O^+]}{K_a} K_{HRCD}[CD]}{\mu_S^0 \mu_{SCD}^0 K_{SCD}[CD] + \mu_{HSCD}^0 \dfrac{[H_3O^+]}{K_a} K_{HSCD}[CD]} \times \frac{1 + K_{SCD}[CD] + \dfrac{[H_3O^+]}{K_a}(1 + K_{HSCD}[CD])}{1 + K_{RCD}[CD] + \dfrac{[H_3O^+]}{K_a}(1 + K_{HRCD}[CD])} \quad (33)$$

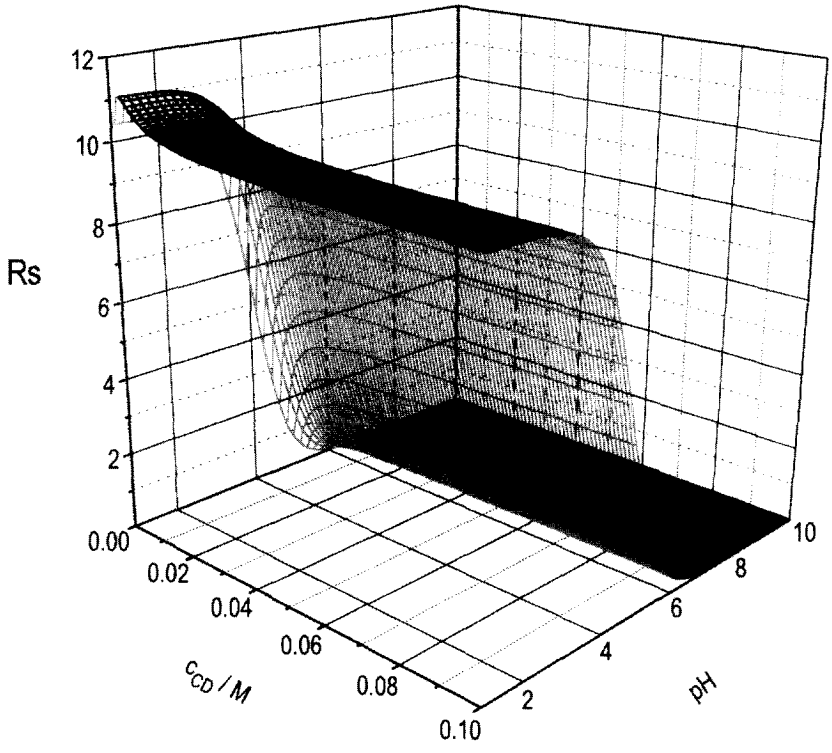

Fig. 10. Peak resolution surface for a weak acid enantiomer pair as a function of the CCD concentration and pH of the BE, when the separation is desionoselective. Constants used for the calculation: $z_R^0 = z_S^0 = 1$, $z_{RCD}^0 = z_{SCD}^0 = 8$, $z_{HRCD}^0 = z_{HSCD}^0 = 7$, $\mu_R^0 = \mu_S^0 = 20 \times 10^{-5}$ cm^2/Vs, $\mu_{RCD}^0 = 30 \times 10^{-5}$ cm^2/Vs, $\mu_{HRCD}^0 = 25 \times 10^{-5}$ cm^2/Vs, $\mu_{HSCD}^0 = 27 \times 10^{-5}$ cm^2/Vs, $K_{RCD} = K_{SCD} = 200$, $K_{HRCD} = 600$, $K_{HSCD} = 660$, $K_a = 5 \times 10^{-5}$, $\beta = 0$.

The z^{eff} and μ^{eff} surfaces for a weak acid analyte are shown in Fig. 7 and Fig. 8. Even for a moderately strongly complexing fully protonated analyte ($K_{HRCD}=600$), z^{eff} and μ^{eff} increase very rapidly, and almost level off for a CCD concentration as low as 20 m*M*. The contribution of the native charge of the analyte to z^{eff} at high pH is comparatively minor vis-a-vis the effects of the CCD. Since the effective charge surface is practically flat over almost all of the useful operating parameter space, its effects on peak resolution will mostly manifest through the simple $(z^{eff})^{1/2}$ multiplier relationship in Eq. (3). Thus, the operating conditions can be selected primarily on the basis of the selectivity surface.

By analyzing Eq. (33) it can be noted that there are three typical, fundamentally different separation types when CCDs are used (similarly to what was observed with neutral cyclodextrins [17–23]). These separation types can be identified as desionoselective, ionoselective and duoselective separations.

In a desionoselective separation, only the nondissociated forms of the enantiomers complex selectively ($K_{RCD}=K_{SCD}$, $K_{HRCD}\neq K_{HSCD}$, $\mu^0_R=\mu^0_S$, $\mu^0_{RCD}=\mu^0_{SCD}$, $\mu^0_{HRCD}\neq\mu^0_{HSCD}$), which simplifies Eq. (33). The resulting selectivity surface is shown in Fig. 9. At a constant, low pH value, well below the pK_a of the analyte, α resembles the simple behavior of a neutral analyte: α decreases as c_{CD} is increased. For a moderately strongly complexing analyte ($K_{HRCD}=600$), the surface almost levels off by the time c_{CD} reaches 20 m*M*. If pH is increased at a constant CCD concentration, α first remains constant, then begins to decrease towards unity as the weak acid becomes increasingly dissociated. Obviously, there is no selectivity at high pH, no matter what the value of c_{CD} is.

The resolution surface (in the absence of EO flow, i.e. at $\beta=0$) is shown in Fig. 10. R_s closely tracks the behavior of α. Due to the rapidly increasing effective charge as c_{CD} is increased, the R_s maxi-

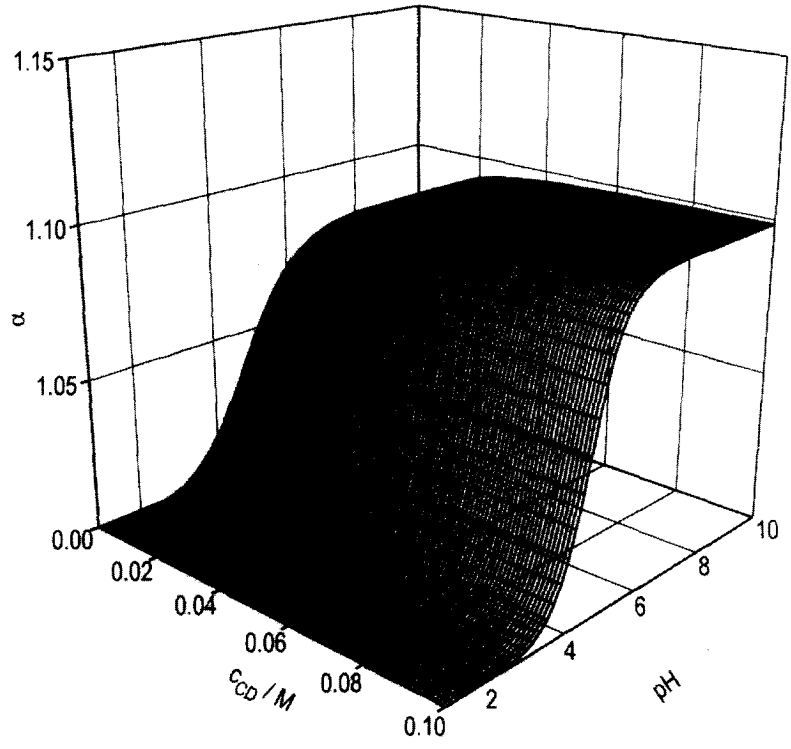

Fig. 11. Separation selectivity surface for a weak acid enantiomer pair as a function of the CCD concentration and pH of the BE, when the separation is ionoselective. Constants used for the calculation: $\mu^0_R=\mu^0_S=20\times10^{-5}$ cm^2/Vs, $\mu^0_{RCD}=30\times10^{-5}$ cm^2/Vs, $\mu^0_{SCD}=33\times10^{-5}$ cm^2/Vs, $\mu^0_{HRCD}=\mu^0_{HSCD}=25\times10^{-5}$ cm^2/Vs, $K_{RCD}=200$, $K_{SCD}=220$, $K_{HRCD}=K_{HSCD}=600$, $K_a=5\times10^{-5}$.

mum is not very sharp. This is advantageous, because it makes for very rugged separations at low pH, at least as long as there is a sufficiently high c_{CD} value. The locus of the R_s maximum depends on the respective values of the complexation constants and ionic mobilities.

In an ionoselective separation only the dissociated forms of the enantiomers complex selectively ($K_{HRCD}=K_{HSCD}$, $K_{RCD}\neq K_{SCD}$, $\mu_R^0=\mu_S^0$, $\mu_{HRCD}^0=\mu_{HSCD}^0$, $\mu_{RCD}^0\neq\mu_{SCD}^0$), which somewhat simplifies Eq. (33). The selectivity surface is shown in Fig. 11. Obviously, there is no selectivity at low pH, irrespective of the concentration of the CCD. At pH values above the pK_a of the enantiomer, α levels off as both pH and c_{CD} are increased.

Since z^{eff} monotonously increases as both the pH and the concentration of the CCD increase, R_s closely follows the behavior of α. The R_s surface (in the absence of EO flow, i.e. at $\beta=0$) is shown in Fig. 12. Very stable, rugged separations can be obtained at high pH and high CCD concentrations.

In a duoselective separation, both the dissociated and the nondissociated forms of the enantiomers complex selectively ($K_{HRCD}\neq K_{HSCD}$, $K_{RCD}\neq K_{SCD}$, $\mu_R^0=\mu_S^0$, $\mu_{HRCD}^0\neq\mu_{HSCD}^0$, $\mu_{RCD}^0\neq\mu_{SCD}^0$), consequently Eq. (33) cannot be simplified. The corresponding selectivity surface is shown in Fig. 13. At low pH, this surface shows the features of a desionoselective separation, at high pH those of an ionoselective separation. The selectivity surface is fairly flat which, in turn, leads to a flat resolution surface when the c_{CD} is sufficiently high, as shown in Fig. 14. Duoselective separations are often very rugged separations.

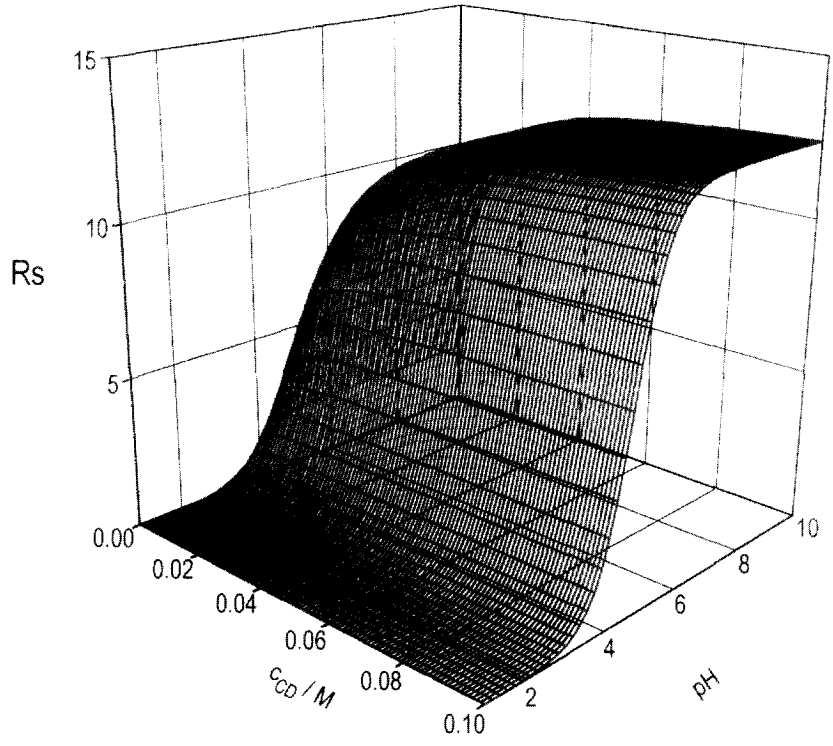

Fig. 12. Peak resolution surface for a weak acid enantiomer pair as a function of the CCD concentration and pH of the BE, when the separation is ionoselective. Constants used for the calculation: $z_R^0=z_S^0=1$, $z_{RCD}^0=z_{SCD}^0=8$, $z_{HRCD}^0=z_{HSCD}^0=7$, $\mu_R^0=\mu_S^0=20\times10^{-5}$ cm^2/Vs, $\mu_{RCD}^0=30\times10^{-5}$ cm^2/Vs, $\mu_{SCD}^0=33\times10^{-5}$ cm^2/Vs, $\mu_{HRCD}^0=\mu_{HSCD}^0=25\times10^{-5}$ cm^2/Vs, $K_{RCD}=200$, $K_{SCD}=220$, $K_{HRCD}=K_{HSCD}=600$, $K_a=5\times10^{-5}$ and $\beta=0$.

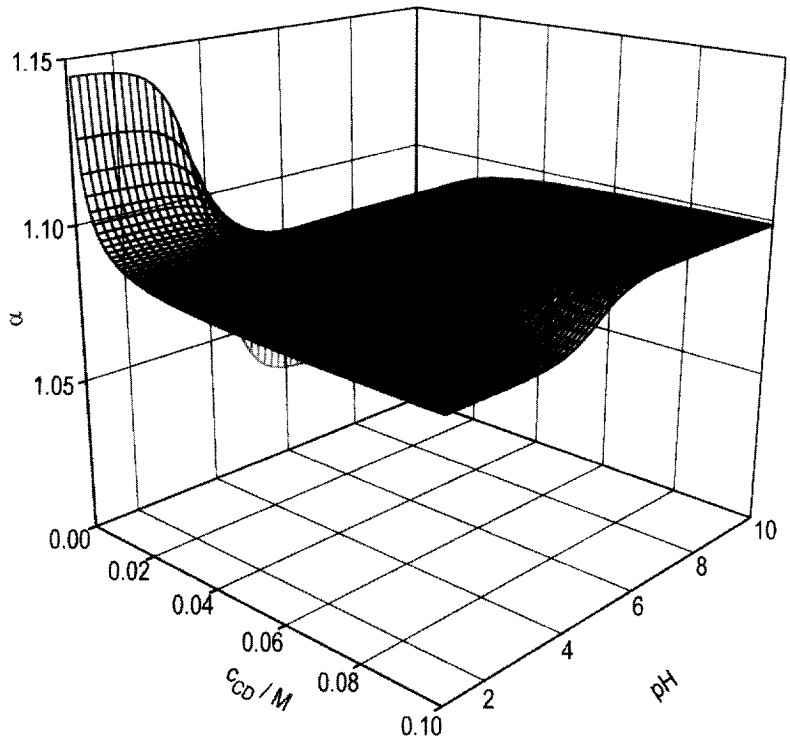

Fig. 13. Separation selectivity surface for a weak acid enantiomer pair as a function of the CCD concentration and pH of the BE, when the separation is duoselective. Constants used for the calculation: $\mu_R^0=\mu_S^0=20\times10^{-5}$ cm^2/Vs, $\mu_{RCD}^0=30\times10^{-5}$ cm^2/Vs, $\mu_{SCD}^0=33\times10^{-5}$ cm^2/Vs, $\mu_{HRCD}^0=25\times10^{-5}$ cm^2/Vs, $\mu_{HSCD}^0=27\times10^{-5}$ cm^2/Vs, $K_{RCD}=200$, $K_{SCD}=220$, $K_{HRCD}=600$, $K_{HSCD}=660$, $K_a=5\times10^{-5}$.

3. Conclusions

The current molecular-level understanding of the enantio-resolution process is inadequate for the a priori selection of the best resolving agent for a particular chiral analyte. Therefore, the most crucial step in the development of a chiral CE separation method, the selection of the resolving agent, is not as predictable as one would like it to be. In fact, selection of the resolving agent from a reasonably broad set of chiral BE additives (offering sufficiently different intermolecular interactions), is a matter of trial-and-error. However, the CHARM model, as described above, can help with the rational and predictable selection of the operating conditions.

Eq. (3) indicates that, as long as their enantioselective interactions are similar, highly charged resolving agents lead to greater R_s values and faster separations than neutral resolving agents do. Since R_s strongly depends on the value of the normalized EO flow (Eq. (3)), it is easiest to begin the method development work with a capillary that does not have EO flow either at low pH or high pH.

With strong electrolyte-type, multiply charged chiral resolving agents, in the absence of EO flow, the peak resolution values for neutral and permanently charged analytes are similar at all pH values. For weak electrolyte analytes, resolution is high at low pH for the desionoselective separation of weak acids and the ionoselective separation of weak bases. Resolution is high at high pH for the ionoselective separation of weak acids and the desionoselective separation of weak bases. Resolution is high both at low pH and high pH for the duoselective separation of both weak acids and weak bases. Therefore, efficient method development requires the use of only two BEs: one at low pH (e.g. pH 2.2) and one at high pH (e.g. pH 9.5 or above).

Since most resolution surfaces level off with increasing concentrations of the CCD, initial runs

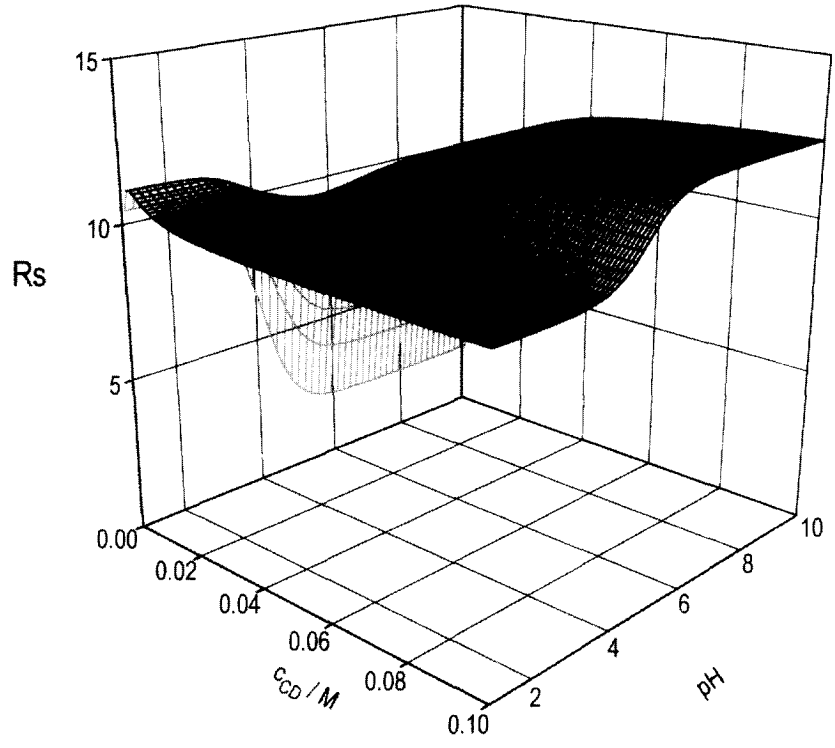

Fig. 14. Peak resolution surface for a weak acid enantiomer pair as a function of the CCD concentration and pH of the BE, when the separation is desionoselective. Constants used for the calculation: $z^0_R = z^0_S = 1$, $z^0_{RCD} = z^0_{SCD} = 8$, $z^0_{HRCD} = z^0_{HSCD} = 7$, $\mu^0_R = \mu^0_S = 20 \times 10^{-5}$ cm^2/Vs, $\mu^0_{RCD} = 30 \times 10^{-5}$ cm^2/Vs, $\mu^0_{RCD} = 33 \times 10^{-5}$ cm^2/Vs, $\mu^0_{HRCD} = 25 \times 10^{-5}$ cm^2/Vs, $\mu^0_{HSCD} = 27 \times 10^{-5}$ cm^2/Vs, $K_{RCD} = 200$, $K_{SCD} = 220$, $K_{HRCD} = 600$, $K_{HSCD} = 660$, $K_a = 5 \times 10^{-5}$ and $\beta = 0$.

should be made at both pH values with a moderate resolving agent concentration. If the observed resolution is inadequate, the concentration of the CCD may be varied in both the low pH and the high pH BEs to locate the R_s maximum point (Figs. 3,10,12 and 14).

One word of caveat is in order, though, with the oppositely charged resolving agents and analytes: the sign of the effective charge of the analyte cannot be predicted a priori: either cathodic or anodic migration could occur depending on the values of the complexation constants. If no peaks show up under normal conditions, an injection from the detector side of the capillary can be made to verify that opposite run polarities are needed.

In the absence of EO flow, the experimentally observed mobilities derived from scouting runs can be interpreted easily, and the approximate extent of complexation between the resolving agents and the analytes can be deciphered quickly. Once a promising resolving agent is found, the EO flow-rate can be varied by changing the nature of the wall of the capillary (uncoated vs. neutral coated vs. anionically coated vs. cationically coated capillary wall), to predictably improve peak resolution, speed up the separation or alter the migration order of the enantiomers, as demanded by the objectives of the separation. This often results in increased separation times. At the present state of the art, it is not easy to predict how much the β value will change as the nature of the capillary wall is changed. Nevertheless, perseverance and some luck can lead to more desirable β values.

Often, electromigration dispersion leads to peaks that are very broad: tailing or fronting. In fact, in our experience, failure in enantiomer separations is often caused by mismatched mobilities. The extent of electromigration dispersion can be mitigated by

increasing the ionic strength of the BE, or by using a mobility matching buffer [26,27].

When all else fails, one can turn to organic cosolvents and/or additional BE modifiers (e.g. micellar agents, multiple resolving agents, etc.) However, these measures do not produce a priori predictable improvements in the separation, and reintroduce the element of art into the science of enantiomer separations.

In final conclusion, our experience is that as long as the analyte can be dissolved in a BE, it is a lot easier to develop a workable CE enantiomer separation than a comparatively useful HPLC separation. In light of the advantages of charged resolving agents, we anticipate an explosive growth in their use in CE.

Acknowledgments

Partial financial support of this project by the Advanced Research Program of the Texas Coordinating Board of Higher Education (Grant No. 010366-016), Beckman Instruments (Fullerton, CA) and the R.W. Johnson Pharmaceutical Research Institute (Spring House, PA) is gratefully acknowledged.

References

[1] R.L. St. Claire, Anal. Chem. 68 (1996) 569R.
[2] S. Fanali, J. Chromatogr. A 735 (1996) 77.
[3] S. Terabe, Trends Anal. Chem. 8 (1989) 129.
[4] S. Fanali, J. Chromatogr. 474 (1989) 441.
[5] T. Schmitt, H. Engelhardt, Chromatographia 37 (1993) 475.
[6] R.J. Tait, D.J. Skanchy, D.O. Thompson, N.C. Chetwyn, D.A. Dunshee, R.A. Rajewsky, V.J. Stella, J.F. Stobaugh, J. Pharm. Biomed. Anal. 10 (1992) 615.
[7] R.J. Tait, D.O. Thompson, J.F. Stobaugh, Anal. Chem. 66 (1994) 4013.
[8] C. Dette, S. Ebel, S. Terabe, Electrophoresis 15 (1994) 799.
[9] W.H. Wu, A.M. Stalcup, J. Liq. Chromatogr. 18 (1995) 1289.
[10] C. Desiderio, S. Fanali, J. Chromatogr. A 716 (1996) 183.
[11] B. Chakvetadze, G. Endresz, G. Blaschke, Electrophoresis 15 (1994) 804.
[12] B. Chakvetadze, G. Endresz, G. Blaschke, J. Chromatogr. A 704 (1995) 234.
[13] A.M. Stalcup, K.H. Gahm, Anal. Chem. 68 (1996) 1360.
[14] S.A.C. Wren, R.C. Rowe, J. Chromatogr. 603 (1992) 235.
[15] S.A.C. Wren, R.C. Rowe, J. Chromatogr. 609 (1992) 363.
[16] S.A.C. Wren, R.C. Rowe, J. Chromatogr. 635 (1993) 113.
[17] Y.Y. Rawjee, D.U. Staerk, Gy. Vigh, J. Chromatogr. 635 (1993) 291.
[18] Y.Y. Rawjee, R.L. Williams, Gy. Vigh, J. Chromatogr. A 652 (1993) 233.
[19] Y.Y. Rawjee, Gy. Vigh, Anal. Chem. 66 (1994) 428.
[20] Y.Y. Rawjee, R.L. Williams, Gy. Vigh, J. Chromatogr. A. 680 (1994) 599.
[21] Y.Y. Rawjee, R.L. Williams, L.E. Buckingham, Gy. Vigh, J. Chromatogr. A. 688 (1994) 273.
[22] M.L. Biggin, L.E. Buckingham, Gy. Vigh, J. Chromatogr. A. 692 (1995) 319.
[23] R.L. Williams, Gy. Vigh, J. Chromatogr. A. 716 (1995) 197.
[24] W. Friedl, E. Kenndler, Anal. Chem. 65 (1993) 2003.
[25] A. Tisielius, Nova Acta Regiae Soc. Sci. Ups. 4 (1930) 4.
[26] R.L. Williams, G.y. Vigh, J. Chromatogr. A. 744 (1996) 75.
[27] R.L. Williams, Gy. Vigh, J. Chromatogr. A 763 (1997) 253.